Line shape of beam deflection of magnetic nanoparticles in a Stern-Gerlach setup

Rajib Kumar Das and Aniruddha Konar
Department of Physics, Indian Institute of Technology, Kanpur, Uttar Pradesh 208016, India

Sushanta Dattagupta
Nano Science Unit, S.N. Bose National Centre for Basic Sciences, JD Block, Sector III, Salt Lake City, Kolkata 700098, India
(Received 22 July 2004; published 31 January 2005)

An adaptation of the famous Stern-Gerlach experiment has found important applications to nanomagnetism. A beam of magnetic clusters is sent in a projectile through an inhomogeneous magnetic field and the resultant deflected spots are collected on a detector screen. The difference with the historic experiment is that the beam deflection during the traversal through the magnetic region is influenced by rotational diffusion of the magnetization vector across an anisotropy barrier. In this paper we provide a complete analysis of the line profile of the deflected spots and a detailed comparison with experimental data.

DOI: 10.1103/PhysRevB.71.014442 PACS number(s): 75.60.Lr

I. INTRODUCTION

Interest in single-domain magnetic nanoparticles has been rekindled in view of the recent upsurge of the importance of nanotechnology.[1] These particles are usually about 1 nm in diameter and possess a giant magnetic moment because of the large cluster ($\sim 10^3$ atoms) of magnetic moments being coherently locked together.[2] However, the direction of the magnetic moment is not fixed in space as thermal fluctuations cause it to fluctuate in time as it undergoes rotational Brownian motion over an anisotropy energy barrier.[3] The characteristic time for rotational relaxation of the magnetization vector, called the Néel relaxation time τ, depends exponentially on the volume V and an anisotropy parameter.[4] Thus, τ is a very sensitive function of the size distribution of the magnetic nanoparticles. When τ is larger than the typical experimental time scale τ_E, the moments are "locked" whereas for τ smaller than τ_E, the particles exhibit magnetic viscosity or superparamagnetism. This interplay of τ and τ_E leads to interesting relaxation behavior[5] and history-dependent effects[6] that can have important applications to magnetic memory devices.

One technique of studying magnetic nanoparticles is to employ the celebrated Stern-Gerlach setup, as shown in Fig. 1, which also introduces some pertinent length scales. Instead of directing a beam of silver atoms through an inhomogeneous magnetic field, as in the historic experiment, what is jettisoned from a hot oven is a beam of clusters that are single-domain magnetic particles.[7] As the beam traverses through the inhomogeneous magnetic field for a time $\tau_E(=L/v)$, v being the speed of the jet in the forward direction, the barycentric motion is accelerated in the transverse direction, which is also the direction of the inhomogeneity of the field. The acceleration, however, is a stochastic process because the mechanical force on the particle depends on the relative angle (between the field and the magnetization), which is a stochastic process, in view of the rotational relaxation phenomenon mentioned above. This in turn makes the deflection of the beam in the transverse direction a stochastic process. The purpose of this paper is to calculate the probability distribution of the spots at which the beam impacts the screen i.e., the line shape of the profile of deflections around their mean.

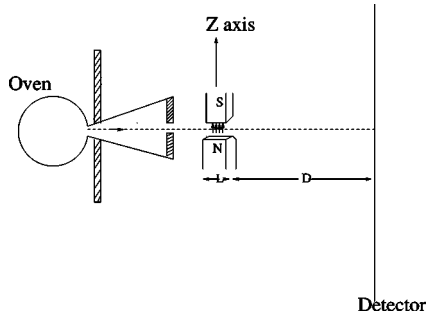

FIG. 1. A typical Stern-Gerlach experimental setup.

In a previous paper (henceforth referred to as I), we computed the mean deflection with the aid of a Fokker-Planck equation for the probability distribution of the angles subtended by the magnetic moment vector along the anisotropy axis.[8] In this paper we extend that theory for evaluating the entire line shape of the deflections in order to facilitate a direct comparison with experiments. While presenting the theoretical results, we stay faithfully close to the experimental paper of Douglass *et al.* (henceforth referred to as II), which provides a comprehensive review of the conditions under which the measurements are carried out.[9] In the process we delineate the important roles of two distinct temperatures: the temperature of the source (oven) T_s, and the vibration temperature T_v, which characterizes the lattice temperature of the particle inside the magnetic environment.

In Sec. II we continue our work from I and present our theoretical results for the variance of the deflections. Some of the details of the calculation are needed to be given in view of the intricate nature of time ordering of the arguments in the required integrals. In Sec. III we discuss a rather surprising result concerning the validity of the central limit theorem in that we are able to fit the experimental line shapes to Gaussians, which are characterized by just two parameters: the mean deflection and the variance. Our principal conclusions are presented in Sec. IV.

 ©2005 The American Physical Society

II. THEORY

The principal result of I is the mean deflection [cf Eq. (13)] which, in terms of all dimensionless entries, is given by

$$\langle \overline{d} \rangle = p_o + \frac{pl}{2} + (p - p_o)\left(1 - \frac{l}{\alpha}\right)\left[1 - \frac{1}{\alpha}(1 - e^{-\alpha})\right], \quad (1)$$

where

$$p_o = \langle \cos \theta_o \rangle,$$

$$p = \langle \cos \theta \rangle_{\mathrm{eq}},$$

$$l = \frac{L}{D},$$

$$\alpha = \lambda \tau_E, \quad (2)$$

λ being the Néel relaxation rate given by Eq. (11) of I. The initial polarization, i.e., the value of $\langle \cos \theta_0 \rangle$, is governed by the source temperature T_s of the oven. As discussed in I, $\langle \overline{d} \rangle$ has two limiting expressions, one for the "locked moment" case governed by "slow relaxation" and the other for "superparamagnetic" case characterized by "fast relaxation." We may further recall that the equilibrium polarization p, for weak anisotropy appropriate for transition-metal clusters of cobalt, nickel, or iron, is expressed as a Langevin function

$$p = \coth\left(\frac{NB_o\mu_o}{k_B T_v}\right) - \frac{k_B T_v}{NB_o\mu_o}, \quad (3)$$

where N is the number of intracluster atoms, B_o is the homogeneous part of the magnetic field, μ_o is the atomic magnetic moment, and T_v is the so-called vibrational temperature. On the other hand, for large anisotropy as is relevant for rare-earth clusters such as those of gadolinium (and its isotopes), p is given by

$$p = \tanh\left(\frac{NB_o\mu_o}{k_B T_v}\right). \quad (4)$$

The corresponding expressions for p_o are obtained by replacing T_v by T_s in Eqs. (3) and (4).

We now go beyond the calculation of the mean deflection, as was done in I, and extend the treatment to evaluate the line shape of the beam deflections. For this purpose the first step is to compute the second moment of the line shape, i.e., the mean square deflection. Before we do that we want to point out one minor modification of the result given in I necessitated by the experimental finding of II. Referring to Fig. 2, which is scanned from the line shape of Co_{115} clusters as given by Fig. 4 of II, we note that while the line shape for the zero magnetic field ($B_o = 0$) and zero inhomogeneity ($B'(0) = 0$) is indeed centered around zero mean deflection, as expected, it is, however, considerably broadened. Since, for zero inhomogeneity, the mechanical force has to vanish, there can be no nonzero magnetic contribution to the second moment. We therefore infer that the observed broadening (for zero magnetic field) has to be attributed to the thermal fluctuation of the velocity of the beam in the transverse (i.e., z) direction (cf. Fig. 1). Thus we write

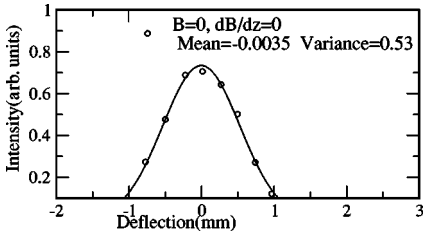

FIG. 2. Deflection profile of Co_{115} clusters at $T_{vib} = 247\ K$ and zero magnetic field, after Fig. 4 of II.

$$v_z(t) = \Delta v_z + b\int_o^t \cos\,\theta(t')dt', \quad (5)$$

where

$$b = \frac{N\mu_o B'(0)}{m}, \quad (6)$$

as defined in I, m being the mass of the cluster, and Δv_z is the pure thermal (kinetic) contribution. It is the second term in Eq. (5) that has led to Eq. (1) above (in which the parameter b has been subsumed in $\overline{d}$) whereas the first term has a zero mean but has a second moment given by the equipartition theorem

$$\langle (\Delta v_z)^2 \rangle = \frac{k_B T_s}{m}. \quad (7)$$

Henceforth we shall ignore the first term in Eq. (5) but remember to add the thermal contribution, Eq. (7) to the computed second moment of the deflection (due purely to magnetic effects) while comparing with experimental data.

Having set aside the issue of residual line broadening we discuss next the deflection d, which, from Eq. (5), can be written as

$$d = \left(\frac{D}{v}\right)v_z(\tau_E) + \int_o^{\tau_E} v_z(t)dt = \left(\frac{bD}{v}\right)\int_o^{\tau_E} \cos\,\theta(t')dt' + b\int_o^{\tau_E} dt \int_0^t \cos\,\theta(t')dt'. \quad (8)$$

In Eq. (8) τ_E is the experimental time scale defined in the second paragraph of sec. I and D is the distance between the magnet and the detector, depicted in Fig. 1. Thus the beam deflection d consists of two contributions: one a single time integral and the other a double time integral of the basic stochastic process, viz., $\cos\,\theta(t)$. The latter has its dynamics governed by a Fokker-Planck equation appropriate to rotational Brownian motion of the orientation of the magnetic moment of a magnetic particle, as mentioned in the beginning of the third paragraph of Sec. I and described in detail in I. Therefore, d itself is a driven stochastic process, the average of which has been computed in I and reproduced in Eq. (1) above.

Our stated objective, as mentioned earlier, is to calculate the line shape of the beam deflection for which we need the knowledge of the mean square deflection, which is given from Eq. (8) by

$$\langle d^2\rangle = \frac{b^2D^2}{v^2}\int_o^{\tau_E} dt' \int_o^{\tau_E} dt''\langle \cos\,\theta(t'')\cos\,\theta(t')\rangle + \frac{2b^2D}{v}\int_0^{\tau_E} dt \int_o^{t} dt' \int_o^{\tau_E} dt''\langle \cos\,\theta(t'')\cos\,\theta(t')\rangle + b^2\int_o^{\tau_E} dt_1 \int_o^{\tau_E} dt_2 \int_o^{t_1} dt' \int_o^{t_2} dt''\langle \cos\,\theta(t'')\cos\,\theta(t')\rangle, \tag{9}$$

where the angular brackets $\langle\cdots\rangle$ denote the average over the underlying stochastic process, the probability distribution of which follows a Fokker-Planck equation [cf. Eq. (6) of I]. The treatment required for evaluating the multiple integrals in Eq. (9) is relegated to Appendix .

Having rewritten the integrals in Eq. (9) in such forms that t' is ensured to be larger than t'', as discussed in the Appendix, the correlation function can be expressed as[10]

$$\langle \cos\,\theta(t'')\cos\,\theta(t')\rangle = \iint \sin\,\theta'' d\theta'' \sin\,\theta' d\theta' p(\theta'',t'') \times \cos\,\theta' \cos\,\theta'' P(\theta'',t''|\theta',t'), \tag{10}$$

where $p(\theta'',t'')$ is the probability that the angle θ takes the value θ'' at time t'' and $P(\theta'',t''|\theta',t')$ is the conditional probability that given the angle to be θ'' at time t'', θ assumes the value θ' at the time $t'(t'>t'')$. As mentioned earlier, it is the function $P(\theta'',t''|\theta',t')$ that obeys a Fokker-Planck equation for the rotational relaxation process at hand. Further, when the ratio of the anisotropy energy and the thermal energy (i.e., NK/k_BT) is sufficiently large, the dynamics of the magnetization vector is concentrated near the angles $\theta=0$ and $\theta=\pi$ and the solution of the probability function can be written as[8]

$$P(\theta'',t''|\theta',t') = P_{\rm eq}(\theta') + [\delta(\cos\,\theta'' - \cos\,\theta') - P_{\rm eq}(\theta')]e^{-\lambda(t'-t'')}, \quad t'>t'' \tag{11}$$

where $P_{\rm eq}(\theta')$ is the Boltzmann probability for the equilibrium distribution of the angle θ appropriate for the vibrational temperature T_v, and given by Eq. (7) of I. It may be noted that the probability function is taken to depend only on the time difference $(t'-t'')$ reflecting the fact that the underlying process is stationary (and Markovian). We may then set $(t'-t'')=\tau$ and identify the epoch $\tau=0$ with the time at which the beam just enters the magnetic region. Hence, the angle θ'' entering the argument of $p(\theta'',t'')$ in Eq. (10) can be taken as the initial projection of the magnetic moment; concomitantly

$$p(\theta'',t'') = p_s(\theta_o), \tag{12}$$

independent of t'', where s stands for "source."

Collecting all the terms, the correlation function in Eq. (10) can be rewritten as

$$\langle \cos\,\theta(t'')\cos\,\theta(t')\rangle \equiv C(\tau) = \langle\cos^2\theta_o\rangle e^{-\lambda\tau} + p_o p(1-e^{-\lambda\tau}), \quad \tau = t'-t''. \tag{13}$$

Substituting in Eq. (9), we obtain

$$\langle \overline{d^2}\rangle = l^2\int_o^{\tau_E} d\tau(\tau_E-\tau)C(\tau) + 2l\int_o^{\tau_E} dt\int_t^{\tau_E} dt'\int_{t'-t}^{t'} C(\tau)d\tau + 4l\int_o^{\tau_E} dt\int_o^{t} dt'\int_o^{t'} C(\tau)d\tau + \int_o^{\tau_E} dt_1\int_o^{t_1} dt_2\int_{t_2}^{t_1} dt'\int_{t'-t_2}^{t'} C(\tau)d\tau + \int_o^{\tau_E} dt_1\int_o^{t_1} dt_2\int_o^{t_2} dt'\int_o^{t'} C(\tau)d\tau, \tag{14}$$

where

$$\overline{d^2} = \frac{d^2}{b\tau_E{}^2 l}. \tag{15}$$

Using the expression for the correlation function $C(\tau)$, given by Eq. (13), the mean deflection $\langle\overline{d}\rangle$ in Eq. (1) and after some straightforward but tedious algebra, the variance of the deflection is derived as

$$\langle(\Delta\overline{d})^2\rangle \equiv \langle\overline{d^2}\rangle - \langle\overline{d}\rangle^2 = 2\left[\frac{pp_o}{2} + \{\overline{p_o} - pp_o\}\left\{\frac{1}{\alpha} - \frac{1}{\alpha^2}(1-e^{-\alpha})\right\}\right] + l\left[\frac{pp_o}{2} + \{\overline{p_o} - pp_o\}\left\{\frac{2e^{-\alpha}}{\alpha^2} + \frac{2}{\alpha} - \frac{2}{\alpha^2}\right\}\right] + l^2\left[\frac{pp_o}{4} + \{\overline{p_o} - pp_o\}\left\{\frac{2}{3\alpha} - \frac{1}{\alpha^2} - \frac{2e^{-\alpha}}{\alpha^3} - \frac{2}{\alpha^4}(e^{-\alpha}-1)\right\}\right] - \left[\frac{p_o}{\alpha}\left\{(1-e^{-\alpha}) + \frac{l}{\alpha}(\alpha+e^{-\alpha}-1)\right\} + \frac{pl}{\alpha}\left\{\frac{\alpha}{2} + \frac{1}{l\alpha}(\alpha-l)(\alpha+e^{-\alpha}-1)\right\}\right]^2, \tag{16}$$

where the symbols have their usual meanings as defined before and $\overline{p_o} \equiv \langle \cos^2\theta_0 \rangle$.

In Eq. (16), nothing has been assumed about either $p_0 = \langle \cos\theta_0 \rangle$ or $\overline{p_o} = \langle \cos^2\theta_0 \rangle$, which can have different values depending on whether the beam is polarized, unpolarized, or partially polarized. In every state of the beam we can also examine Eq. (16) in both slow and fast relaxation regimes.

A. Polarized Beam

In this case $p_0 = \overline{p_o} = 1$. (i) Fast relaxation ($\lambda \tau_E \gg 1$): In this limit the variance of the deflection profile is given by

$$\langle (\Delta \overline{d})^2 \rangle = 2\left[\frac{p}{2} + (1-p)\left(\frac{1}{\alpha} - \frac{1}{\alpha^2}\right)\right] + l\left[\frac{p}{2} + 2(1-p) \times \left(\frac{1}{\alpha} - \frac{1}{\alpha^2}\right)\right] + l^2\left[(1-p)\left(-\frac{1}{\alpha^2} + \frac{2}{3\alpha} + \frac{2}{\alpha^4}\right) + \frac{p}{4}\right] - \left[\left(1 + \frac{l}{2}\right)p + \frac{1}{\alpha}(1+l)(1-p)\right]^2. \quad (17)$$

(ii) Slow relaxation ($\lambda \tau_E \ll 1$)

$$\langle (\Delta \overline{d})^2 \rangle = 1 + l\left(1 - \frac{p}{2}\right) + \frac{l^2}{4} - \left\{\left(1 + \frac{l}{2}\right) - \frac{\alpha}{2}\left[\left(1 + \frac{l}{3}\right)(1-p)\right]\right\}^2. \quad (18)$$

B. Unpolarized Beam

In this case $\langle \cos\theta_0 \rangle = 0$, but

$$\overline{p_o} = \langle \cos^2\theta \rangle = \int_0^\pi \cos^2\theta_0 \sin\theta_0 d\theta_0 = \frac{1}{3}. \quad (19)$$

Therefore, for (i) slow relaxation

$$\langle (\Delta \overline{d})^2 \rangle = \frac{l^2}{12} + \frac{l}{3} + \frac{1}{3} - \frac{p^2\alpha^2}{4}\left(1 + \frac{l}{3}\right)^2, \quad (20)$$

and (ii) fast relaxation

$$\langle (\Delta \overline{d})^2 \rangle = \frac{2}{3}l\left(\frac{1}{\alpha} - \frac{1}{\alpha^2}\right) + \frac{2}{3}l^2\left(\frac{1}{3\alpha} - \frac{1}{2\alpha^2} + \frac{1}{\alpha^4}\right) + \frac{2}{3}\left(\frac{1}{\alpha} - \frac{1}{\alpha^2}\right) - p^2\left[\left(1 + \frac{l}{2}\right) - \frac{1}{\alpha}(1+l)\right]^2. \quad (21)$$

In reality the initial beam may be partially polarized (see II).

III. COMPARISON WITH EXPERIMENTS

As mentioned in Sec. I and discussed further below, we are able to fit the experimentally observed line shapes for the deflection to a Gaussian:

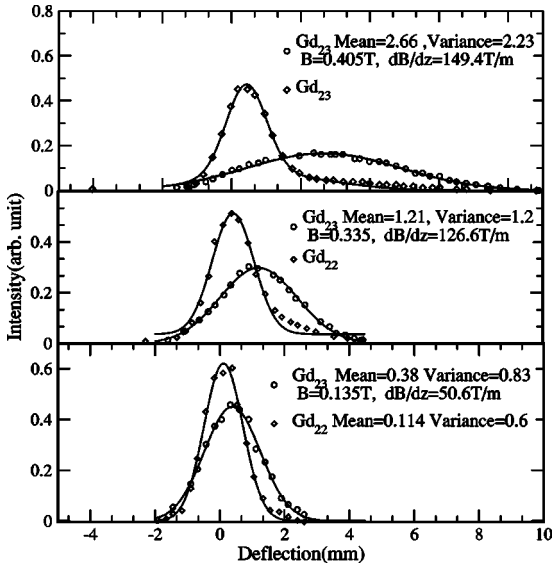

FIG. 3. Deflection profiles of Gd_{22} and Gd_{23} clusters fitted with the Gaussian model of Eq. (22). All experimental (cf. II) curves are indicated by circles and squares appropriate to $T_{vib} = 147$ K.

$$I(\overline{d}) = \frac{1}{\sqrt{2\pi\langle (\Delta \overline{d})^2 \rangle}} e^{-[(\overline{d} - \langle \overline{d} \rangle)^2]/[2\langle (\Delta \overline{d})^2 \rangle]}. \quad (22)$$

Thus only two parameters, the mean deflection $\langle \overline{d} \rangle$ and its variance $\langle (\Delta \overline{d})^2 \rangle$, are required to characterize the measured profiles, both in the locked moment as well as the superparamagnetic regimes. The fitting procedure is as follows. We took the deflection profiles of cobalt and gadolinium clusters from the experimental paper of Douglas *et al.* (II) and fitted them to the function

$$f(x) = \frac{a}{\sqrt{2\pi b^2}} e^{-(x-c)^2/(2b^2)}. \quad (23)$$

Note that in addition to the parameters b and c, depicting the width and the mean respectively, we have taken recourse to an additional parameter a in order to adjust the height of the profiles, as the various intensities are measured in arbitrary units. The fitted curves are shown in Fig. 3 and Fig. 4. From the fitted values of b and c, and a comparison with the theoretically computed mean deflection [Eq. (1)] and the variance [Eq. (16)], we can deduce the value of α, for a given $d_o (= b\tau_E{}^2 l)$ and initial polarization, as the value of p can be estimated from the vibrational temperature T_v of the clusters. A knowledge of $\alpha (= \lambda \tau_E)$ yields important data for the anisotropy parameter of the single-domain cluster.

Turning to the experimental data for Gd_{22} at high magnetic fields (see II and Fig. 5 in the text), we notice a two-peak structure of the profile. Because $\langle \overline{d} \rangle$ and $\langle \overline{d^2} \rangle$ depend on the relaxation rate λ (through the dependence on α), which, in turn, depends exponentially on the size of the cluster (cf. I), we surmise that the sample of Gd_{22} consists of two characteristic cluster sizes. One size yields the locked-moment

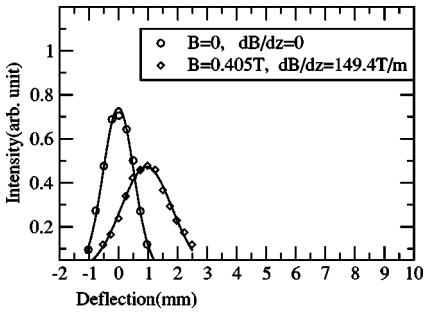

FIG. 4. The deflection profiles of cobalt clusters at different magnetic fields fitted with the Gaussian function of Eq. (22). The unfilled circles and the squares are from the experimental data of II.

behavior appropriate to slow relaxation while the other size leads to superparamagnetic behavior in accordance with fast relaxation. This interpretation, based on bidispersity of clusters, which is consistent with II, is further verified by fitting the experimental line shape to two Gaussians, as shown in Fig. 5. Naturally the second peak which shows up as a shoulder is discernible only at high magnetic fields because the corresponding Zeeman energy also appears in the exponent of λ.

Finally, we may point out that the dependence of the width of the profile linearly on the inhomogeneity $B'(0)$ of the magnetic field [cf. Eqs. (6) and (15)] is also borne out by the simulation data of de Heer *et al.*.[11]

IV. CONCLUSION

The Stern-Gerlach measurement of magnetic deflection of a beam of single-domain magnetic nanoparticles is a useful and complementary technique (to susceptibility,[12] Mössbauer spectroscopy,[13] etc.) for extracting important parameters, e.g., the anisotropy barrier, size dependence of Néel relaxation, magnetic polarization, etc. It also allows elucidation of the roles of two distinct temperatures, the temperature T_s of the source (or the oven) from which the beam is ejected, and the vibration temperature T_v which characterizes thermal equilibration via lattice phonons. In this paper, we show how these parameters can be evaluated by fitting the experimental data to a theoretically computed line shape of the beam deflections.

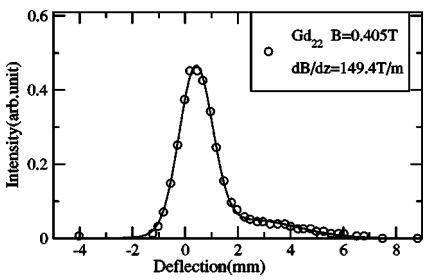

FIG. 5. Experimental (circles) (cf. II) deflection profile of Gd_{22} clusters, which shows two peaks due to bidispersive nature, is fitted with the superposition of two Gaussian functions (solid lines) [Eq. (22)] appropriate to $T_{vib}=147$ K.

While fitting the data, we come across an unexpected finding in that the line shapes are Gaussian. This implies that only two parameters—the variance, which is the cumulant of the second moment of the deflection, and the mean deflection—are adequate for a satisfactory analysis of the experimental results. In the theory of ordinary Brownian motion the velocity of the tagged particle, which is the basic stochastic process, is a stationary Gaussian-Markov process.[14] The displacement, which is the time integral of the velocity, is a *driven* stochastic process and its probability distribution, with open boundary conditions, does turn out to be a Gaussian. In the present case, however, the driven stochastic variable, viz., the beam deflection, is a *double* time integral of the basic stochastic process, i.e., $\cos\theta(t)$. Thus, it is not obvious why the line profile of the beam deflection should end up being a Gaussian, especially when we solve the underlying Fokker-Planck equation approximately, in the Kramers' regime (see I). This point can of course be checked by showing that all cumulants of the deflection, higher than the second, vanish; however, that calculation is very cumbersome and not attempted here.

The analysis presented in this paper demonstrates the usefulness of the Stern-Gerlach setup in studying rotational relaxation of the magnetization of clusters. It would be interesting to extend the investigation to very low vibrational temperatures at which the magnetization is expected to quantum-mechanically tunnel rather than get thermally activated to a different configuration.[15]

ACKNOWLEDGMENTS

Two of us (R.K.D. and A.K.) carried out this project at the SN Bose Centre. We are grateful to our fellow colleagues at the Centre for their-warm hospitality. The authors would like to acknowledge the Department of Science and Technology for its support through the "Nanoscience Initiatives," and Kamal Saha and P. A. Sreeram for their help in curve fittings.

APPENDIX

In order to evaluate the integrals in Eq. (9) we need to time order the arguments t' and t''. For instance, if we want $t'>t''$ time ordering would lead to

$$\int_o^{\tau_E} dt' \int_o^{\tau_E} dt'' \langle \cos\theta(t'')\cos\theta(t')\rangle = 2\int_o^{\tau_E} dt' \int_o^{t'} dt'' \langle \cos\theta(t'')\cos\theta(t')\rangle. \tag{A1}$$

Following this idea, the second term on the right-hand side of Eq. (8) can be decomposed as

$$\int_o^{\tau_E} dt \int_o^{t} dt' \int_o^{\tau_E} dt'' = \int_o^{\tau_E} dt \int_o^{t} dt' \int_o^{t} dt'' + \int_o^{\tau_E} dt \int_o^{t} dt' \int_t^{\tau_E} dt'' = 2\int_o^{\tau_E} dt \int_o^{t} dt' \int_o^{t'} dt'' + \int_o^{\tau_E} dt \int_t^{\tau_E} dt' \int_o^{t} dt'', \tag{A2}$$

where in the last term we have interchanged t' and t'' and used the fact that the correlation function is symmetric in t' and t''. Finally the third term can be manipulated as follows:

$$\begin{aligned}\int_o^{\tau_E} dt_1 \int_o^{\tau_E} dt_2 \int_o^{t_1} dt' \int_o^{t_2} dt'' &= 2\int_o^{\tau_E} dt_1 \int_o^{t_1} dt_2 \int_o^{t_1} dt' \int_o^{t_2} dt'' \\ &= 2\int_o^{\tau_E} dt_1 \int_o^{t_1} dt_2 \left[\int_o^{t_2} dt' \int_o^{t_2} dt'' + \int_{t_2}^{t_1} dt' \int_o^{t_2} dt'' \right] \\ &= 4\int_o^{\tau_E} dt_1 \int_o^{t_1} dt_2 \int_o^{t_2} dt' \int_o^{t'} dt'' \\ &\quad + 2\int_o^{\tau_E} dt_1 \int_o^{t_1} dt_2 \int_{t_2}^{t_1} dt' \int_o^{t_2} dt''. \end{aligned} \tag{A3}$$

[1] A. N. Goldstein, *Handbook of Nanophase Materials* (Marcel Dekker Inc. New York 1997).

[2] I. S. Jacobs and C. P. Bean, in *Magnetism (III)*, edited by G. T. Rado and H Suhl (Academic, New York 1963).

[3] W. F. Brown, Jr., Phys. Rev. **130**, 1677 (1963).

[4] L. Néel, Ann. Geophys. (C.N.R.S.) **5**, 99 (1949); Adv. Phys. **4**, 191 (1955).

[5] E. P. Wohlfarth, J. Phys. F: Met. Phys. **10**, L 241 (1980); R. Street and J. C. Woolley, Proc. Phys. Soc., London, Sect. A **62**, 562 (1949).

[6] S. Chakraverty, M. Bandyopadhyay, S. Chatterjee, S. Dattagupta, A. Frydman, S. Sengupta, and P. A. Sreeram, Phys. Rev. B (to be published).

[7] J. P. Bucher, D. C. Douglass, and L. A. Bloomfield, Rev. Sci. Instrum. **63**, 5667 (1992).

[8] S. Dattagupta and S. D. Mahanti, Phys. Rev. B **57**, 10 244 (1998), henceforth referred to as I.

[9] D. C. Douglass, J. P. Bucher, and L. A. Bloomfield, Phys. Rev. Lett. **68**, 1774 (1992); D. C. Douglass, A. J. Cox, J. P. Bucher, and L. A. Bloomfield, Phys. Rev. B **47**, 12 874 (1993), henceforth referred to as II.

[10] S. Dattagupta, *Relaxation Phenomena in Condensed Matter Physics* (Academic, Orlando, 1987), Chaps. XII and XIII.

[11] W. A. de Heer, P. Milani, and A. Châtelain, Phys. Rev. Lett. **65**, 488 (1990).

[12] D. Kumar and S. Dattagupta, J. Phys. C **16**, 3779 (1983).

[13] See, for instance, M. F. Hansen, C. B. Koch, and S. Morup, Phys. Rev. B **62**, 1124 (2000).

[14] S. Chandrasekhar, Rev. Mod. Phys. **15**, 1 (1943).

[15] See, for instance, P. C. E. Stamp, E. M. Chudnovsky, and B. Barbara, Int. J. Mod. Phys. B **6**, 1355 (1992).